



West Virginia University
National Research Center for Alternative Fuels, Engines, and Emissions

Gregory J. Thompson, Ph.D.
West Virginia University
Department of Mechanical and Aerospace Engineering
P.O. Box 6106
Morgantown WV 26506-6106
Phone: (304) 293-3111 ext. 2481; Fax: (304) 293-6689

SCX, Inc. Ferry Emissions Tests

Final Data Report

Presented to:

Chris Tennant, Ph.D.
National Renewable Energy Laboratory

Prepared by:

Gregory Thompson
West Virginia University
September 5, 2003





Introduction

In-use brake-specific mass exhaust emissions rates were determined for a high-speed hydrofoil ferryboat, the WaveRider. This vessel operates between Oceanside and San Diego, CA as a passenger ferrying service for commuters living north of San Diego. The ferry operates a single round-trip service during the weekday, departing from Oceanside in the morning to arrive in San Diego for the morning commute, and then leaving San Diego in the evening for a return trip to Oceanside. The vessel employs a retractable hydrofoil to achieve high speeds. A picture of the WaveRider is shown in Figure 1 with the hydrofoil deployed. The ferry is approximately 80 feet in length and is powered by four high-speed Detroit Diesel 12V92 compression ignition engines.



Figure 1 The SCX, Inc. WaveRider ferry.

Two of the engines are located on the port side and the other two are located on the starboard side. Each set of engines is connected to a gearbox, that is, the two port engines are connected to a gearbox and the two starboard engines are connected to a second gearbox. The output shaft from each gearbox is used to drive a water jet propulsion system. For each set of engines, one is located fore and the other is located aft in a staggered arrangement. Figure 2 presents a photograph of the forward starboard engine and Figure 3 illustrates the starboard engine pair. The engines incorporate two turbochargers, located on either side of the engine. The outlet of the turbocharger feeds two superchargers. A water injection system (intake fumigation) is incorporated between the turbocharger outlet and supercharger inlet. The water injection control was such that the system was deactivated if the manifold air pressure was below a certain value. Therefore, no water injection data is available for the idle and marina set points. Water is also injected in the exhaust to reduce exhaust system temperatures. The water is injected down stream of the turbocharger outlet, after an elbow as shown in Figure 3.

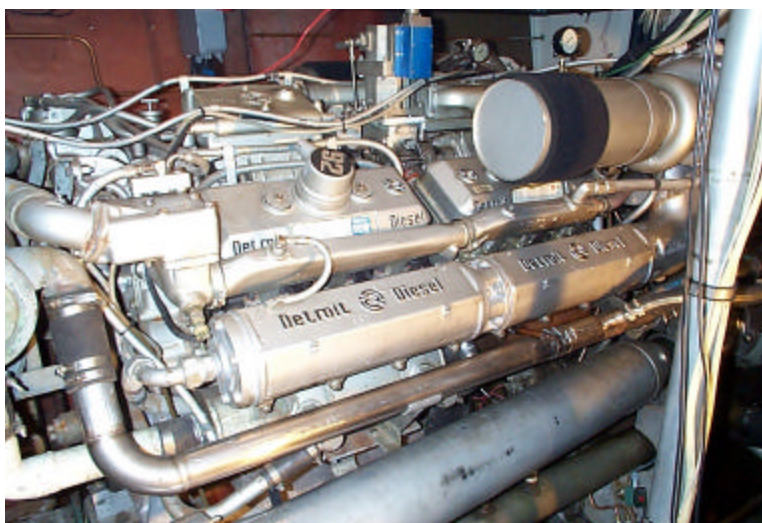


Figure 2 Photograph of the forward starboard engine. The aft engine and gearbox is located behind the engine on the right side of the picture.

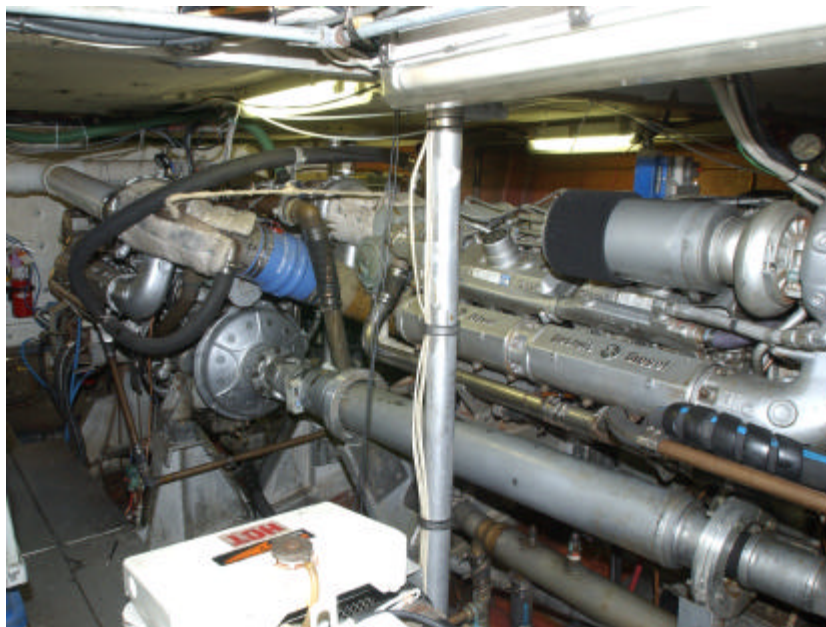


Figure 3 Photograph of the both starboard engines. The forward engine is on the left side of the picture and the aft engine is on the right side. The output shaft of the forward engine is shown in the foreground. A portion of the electrical generator is shown in the bottom of the picture.

The vessel and engines are designed to use conventional marine compression ignition fuel (off-road diesel). Typical marine fuel for high-speed diesel engines is similar to other off-road fuel except that sulfur concentration levels may be as high as 5000 ppm. The fuel was stored in two 800-gallon tanks. Figure 4 shows the return lines and sight gauges for these tanks. There was some uncertainty regarding the exact construction of the fuel storage tanks, but it appears as though the two tanks are constructed from aluminum plates welded together with a center divider plate. It was uncertain if the divider plate separating the two halves were welded at the top, but it was believed to provide adequate separation of the fuel in the two tanks.

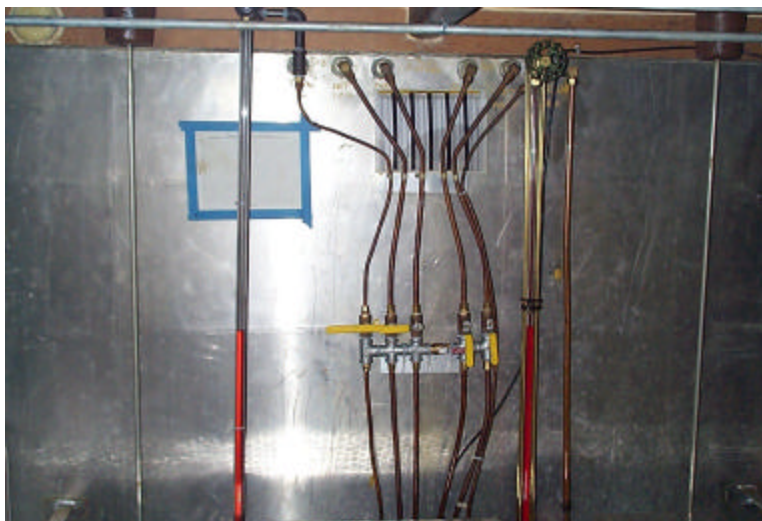


Figure 4 Picture of the fuel tanks and return lines from the four propulsion and electrical generator set. The two sight gauges are seen with the red-dyed fuel.

In an effort to reduce the oxides of nitrogen (NO_x) emissions generated from these engines, a water fumigation system was installed in the intake to add additional humidification. To reduce particulate matter (PM), low sulfur diesel fuel was used in place of the higher sulfur-level marine diesel. The water injection system was supplied and installed by M.A. Turbo/Engine, Ltd. [1]. The low sulfur diesel (LSD) fuel was supplied by BP and is designated as BP ECD[®]. The testing consisted of examining the emissions produced by the starboard, forward engine when it was fueled with marine fuel and with LSD fuel. In addition, for each fuel, the emissions were measured with and without the water injection system activated, thus making a total of four different engine configurations. For each of these four configurations, the engine was operated at four different speeds to evaluate the emissions, namely, idle (650 rpm), 1900 rpm, 2000 rpm, and 2100 rpm.

The purpose of this testing was to determine the differences in exhaust mass emissions from one of the engines while the vessel was operated over steady state test conditions. Gaseous emissions NO_x and carbon dioxide (CO₂) and particulate matter emissions data were collected. The test engine specification is listed in Table 1. All emissions tests were performed on the Pacific Ocean outside the Oceanside marina.

Representatives from SCX, Inc. provided and operated the ferryboats, while West Virginia University (WVU) provided and operated the emissions measurement equipment. Measurements were done while the ferry was not in normal service. The computed results of the emissions tests are presented in this report.



Table 1 Forward starboard test engine specifications.

Engine Manufacturer	Detroit Diesel Corp.
Engine Model	12V92
Model Year	1981
Engine I.D.	12VF002734.5.0.2A83804
Displacement (cu. in.)	1104 in ³
Power Rating (hp)	1080 hp @ 2300 rpm
Configuration	12V92
Bore (in.) x Stroke (in.)	4.84 x 5.00
Induction	Turbocharger with Blower
Fuel Type	Diesel
Engine Strokes per Cycle	Two
Injection	Mechanical

OBJECTIVE

The objective of this study was to measure engine emissions reduction of oxides of nitrogen (NO_x), which resulted from implementation of an intake water injection system, and total particulate matter (TPM), which was afforded by changing from marine diesel (high sulfur) to a lower sulfur fuel. The emissions reduction program was in support of the “Project 81, Governor’s Congestion Relief Program – High Speed Low-emissions Ferry Demonstration” granted to the Unified Port District of San Diego. Fuel consumption (FC) was also measured to determine if there was a fuel penalty associated with either the fuel change or implementation of the water injection system. For this testing, West Virginia University designed and developed a raw emissions sampling system, according to recommendations provided by Title 40 CFR 86, Title 40 CFR 89, Title 40 CFR 92, Title 40 CFR 94, ISO8178, and SAE J177 [2-7], where applicable. The system employed in the collection of the data is explained below.

Overview of Exhaust Emissions Measurement System

The following section is included in order to outline the equipment and procedures used for the evaluation of the ferryboat engine exhaust emissions. Due to space limitations and the nature of in-use emissions testing, particular attention was paid to the selection of the analytical equipment. WVU designed and developed a raw exhaust emissions sampling and measurement system that would provide the highest possible accuracy while following the requirements set forth in Title 40 CFR 86, Title 40 CFR 89, Title 40 CFR 92, Title 40 CFR 94, ISO8178, and SAE J177 [2-7], where applicable. In particular, analyzers and transducers were selected that would provide levels of accuracy specified in the above documents without being adversely affected by the vibrations encountered during normal operation of the ferry.

A. Particulate Sampling System

The primary goal of engine emissions testing was to determine the effects that exhaust constituents have on the environment. In order to simulate “real world” conditions and to produce accurate particulate matter measurements, it was necessary to mimic the dilution process that occurs when hot exhaust gases mix with ambient air. However, it should be noted that for this ferry the raw exhaust is flooded with



water to cool the exhaust and is ported to the side of the vessel at the water line. Therefore, the exhaust from the engines from this vessel never does mix with ambient air, as is the case for most land-based engines. The effects of this exhaust gas dilution are threefold, with the primary reason being provision for exhaust-air interactions that would normally take place at the exhaust outlet. In addition, the dilution process quenches post-cylinder combustion reactions and lowers the exhaust gas dew point, thus inhibiting condensation.

The dilution tunnel used for this research was of a partial-flow design, where a measured amount of exhaust gas emitted by the test engine was routed into the tunnel and mixed with a regulated amount of HEPA-filtered, conditioned dilution air in order to achieve desired dilution ratios. The raw exhaust sample probe is described below. The system was mass-flow controller based, but uses conditioned, time-aligned raw and dilute CO₂ tunnel concentrations to infer dilution ratios and exhaust sample inlet flow rates. The dilution tunnel, which was approximately 2 inches in diameter and 24 inches in length, was constructed of stainless steel to prevent oxidation contamination and degradation. The dilution air supply was provided by a rotary-vane pump, and was HEPA-filtered and cooled to remove water and maintain near-ambient temperatures. The exhaust gases entered the tunnel at its centerline and passed through a mixing orifice plate that was close-coupled to the divergent tunnel entrance. The orifice plate creates turbulence in the flow path that promotes thorough mixing. In addition, tunnel flow rates were maintained sufficiently high so as to promote fully-developed, blunt-shaped turbulent flow profiles that reduce the sensitivity of point-source sample probe placement. The full tunnel flow stream was pulled through a stainless steel filter holder that contains two Pallflex 70mm diameter Model T60A20 fluorocarbon-coated glass microfiber filters in series. Two filters, a primary and a secondary, were used in the filter holder to maximize filter trapping efficiency. The diluted sample stream was maintained at temperatures below 125°F, measured at the inlet of the PM filter holder. The purpose of this was to keep the face of the particulate sample filter at a sufficiently low temperature so as to prevent any physical damage to the filter material or stripping of volatile components that would normally condense upon the filter surface.

Sierra mass flow controllers provided flow rate control of the total flow and dilution air based on computer voltage outputs determined from the raw and dilute CO₂ concentrations. The mass flow controllers were recalibrated by the manufacturer and additionally checked with Merriam Instruments laminar flow elements. As aforementioned, the deduction of dilution ratio was provided through the measurement of dilute and raw CO₂ concentrations in the dilution tunnel. Exhaust sample flow rates into the tunnel were inferred from dilution ratio measurements and total mass flow rates measured with the mass flow controllers. This provided redundant measurements that helped to insure accurate dilution ratio measurements.

The PM from the diluted exhaust stream of the tunnel was used to gravimetrically infer the amount of PM emitted by the engine during a given test cycle. PM collected on the filter consists primarily of elemental carbon as well as sulfates, the soluble organic fractions (SOF), engine wear metals and bound water. The sample filters were conditioned in an environmentally controlled chamber to 70°F and 50% relative humidity, in compliance with requirements of CFR Parts 86 and 89 [2, 3], and weighed before and after sample collection using a Cahn C-32 microbalance. However, for this research effort, the filters were pre-weighed at the Engine and Emissions Research Laboratory (EERL) at WVU and shipped to the test site in individually labeled petri dishes. After the filters were used, they were shipped back to the EERL and reconditioned and the final weight recorded. The required times set forth in CFR Parts 86 and 89 [2, 3] were not followed. However, previous experience with gravimetric PM analyses performed at



remote sites indicates minimal, if any, variations due to non-standard PM conditioning constraints as long as the filters are conditioned for the prescribed amount of time.

B. Gaseous Emission Sampling System

The sampling system originated with stainless-steel sample probes that were mounted in the raw exhaust stack just after the turbocharger. These multi-hole, stainless-steel probes were designed according to the recommendations included in CFR 40 Part 89, Subpart E [3]. Due to the direct injection of water to cool the exhaust and dual turbochargers, exhaust samples were pulled from each engine exhaust bank and merged together to obtain an average engine exhaust composition. Due to the divorced turbocharger arrangement, intake manifold pressures were observed to insure that equal amounts of exhaust flowrates were being supplied from each engine bank so as to prevent measurement bias when using this integrated sampling procedure. Heated sample lines were used from the probe to the measurement system located on the main deck. The wall temperatures of the filter assembly and the heated sample transport lines were electrically heated and maintained at a temperature of $375^{\circ} \pm 10^{\circ}\text{F}$ using electronic temperature controllers. This temperature set point, prescribed by CFR 40, Parts 86 and 89 [2, 3], prevents the high molecular weight hydrocarbons from condensing in the sample line. It is noted that THC's were not measured for this project due to the concerns of needing compressed hydrogen for a flame ionization detector. It is also noted that diesel engines typically have very low HC emissions relative to the other carbon compounds (CO and CO_2) and that only NO_x and PM were the targeted compounds. The heated sample lines transported the exhaust sample to the emissions sample conditioning system. The heated line was again teed with one leg going to the gaseous sampling system and the other leg going to the particulate matter mini dilution tunnel.

This system incorporated a heated filter assembly, a heated-head pump, an external NO_2 converter, flow control devices, and a sample moisture control system. The flow rate controllers were implemented to provide a constant, pulsation-damped sample for the gas analyzers, since sample pressure fluctuations can compromise measurement accuracy. Sample humidity control was used to prevent the interference effects of water – a common problem for non-dispersive infrared (NDIR) gas analyzers.

C. Exhaust Gas Analyzers

The gas analysis bench housed both NO_x and CO_2 analyzers. A brief description of each analyzer and its components, as well as theory of operation is included in this section. The entire sampling system used was compared against a full-scale dilution tunnel and engine dynamometer that conforms to CFR 40 Part 86, Subpart N and Part 89, Subpart D [2, 3]. The basis of the gaseous emissions sampling system is described in more detail elsewhere but is summarized here [8-11].

Oxides of Nitrogen Analyzer

Electrocatalytic analyzers measure oxygen concentrations based on a flow of electrons across a solid zirconium oxide (ZrO_2) catalytic electrolyte. ZrO_2 allows the transfer of O_2 ions when heated to approximately 700°C . A current is generated if the electrolyte is placed between gases of two different concentrations. Oxygen sensors of this type are the standard in the automotive industry for feedback control of air-fuel ratio. This principle may also be used to measure concentrations of other gases. NO is measured by first removing O_2 from the sample and then causing the NO to dissociate into N_2 and O_2 . Oxygen is removed from the sample through a ZrO_2 electrolyte coated with platinum to catalyze the transfer process. Current must be supplied in this case because the oxygen is being transferred in the

opposite direction of the flow that would be induced by the concentration gradient. The sample then flows into a second cavity where the O_2 produced from the dissociation process is measured with a second electrocatalytic device of the same design as the first. Zirconium oxide sensors typically have a T_{90} response time of less than one second for NO. Although zirconium oxide sensors do respond to some NO_2 it is advisable to still use an NO_2 to NO converter to obtain total NO_x measurement. The sample can be filtered to prolong the sensor's life. A Horiba MEXA120 was used for this work.

Electrochemical (EC) or polarographic analyzers are a relatively simple and inexpensive method of measuring concentrations of emission gases including NO, NO_2 , NO_x, SO_2 , CO, O_2 , and CO_2 . An electrochemical cell consists of two or more electrodes separated by an electrolyte. For a cell with two electrodes, one electrode must be porous so the gas can pass through it after diffusing through a membrane. A resistor is connected between the two electrodes and voltage drop across the resistor is converted to gas concentration. If the rate of diffusion is controlled via a membrane, the current flowing through the resistor and therefore, the voltage drop across the resistor is proportional to the concentration of candidate gas, as stated by Fick's law of diffusion. Electrochemical cells typically have a T_{90} response time of at least 5 seconds for NO. An NO_2 to NO converter is required to obtain total NO_x measurement. The sample must be filtered to avoid clogging of the membrane.

The MEXA 120 and EC cells are inherently linear by nature, but the linearized response was validated through calibration curves that were generated before each testing session began. These calibration curves were generated by using a capillary-flow gas divider and component gases mixtures that are traceable to the standards set forth by the National Institute of Standards and Technology (NIST).

Carbon Dioxide Analyzer

Gaseous constituents of CO_2 were measured with a Horiba BE-140 non-dispersive infrared (NDIR) gas analyzer. NDIR analyzers operate using the principle of selective infrared light absorption – where a particular gas will absorb a certain wavelength of light within the infrared spectrum, while the other spectral wavelengths are able to transmit through the gas. The analyzer detects the amount of infrared energy able to pass through the sample gas and uses it in the determination of the concentration of the measured absorbent gas in the sample stream. An NDIR analyzer is inherently non-linear by nature, so linearized calibration curves were generated for the analyzers before each testing session began. These calibration curves were generated by using a capillary-flow gas divider and component gases mixtures that are traceable to the standards set forth by the NIST.

D. Fuel Flow Rate

Continuous direct fuel flow measurements were made using two Micro Motion CMF025 flowmeters with RFT9739D4SUA transmitters. One unit provided information regarding the supply side, while the other unit collected fuel flow rate data for the return side. The calibration constants supplied by the manufacturer for each sensor were entered into the WVU data acquisition (DAQ) program.

E. Intake and Exhaust Flow Rates

Two different means were used to measure or infer the intake and exhaust flow rates through the engine. The first method was a Meriam laminar flow element placed in the intake stream of the engine. The absolute pressure, differential pressure, and exhaust temperatures were recorded and stored with the WVU DAQ. These transducers were calibrated at WVU prior to the testing and the calibration checked

at the test site. The second method was inference of exhaust flow rates through direct fuel flow measurements and carbon balance (CO_2), using exhaust CO_2 measurements.

F. Shaft Speed/Torque

Engine shaft speed and torque was measured using an Advanced Telemetry International Model 2025B-S transmitter and receiver. A radio frequency (RF) signal was transmitted from the shaft in the engine compartment area to the receiver located on the lower deck seating area of the ferry. The signals from the receiver were connected into the WVU DAQ. The load cell for the torque was installed on the existing driveshaft and calibrated on-board using a shaft locking system and dead weights. The calibration of shaft speed was confirmed with the engine speed display.

The method of calibrating the shaft load cell is illustrated in Figure 5. The load cell was installed onto the shaft and is visible on the right-hand side of the left picture. The shaft was locked in place by a fabricated arm that was bolted to the drive flange at the shaft and contacted the hull of the vessel. At the other end of the shaft, before the connection with the transmission, a second fabricated arm was bolted to that drive flange. Pre-weighed weights were then placed on this calibration arm to calibrate the load cell. The response of the load cell was recorded for the known weight.

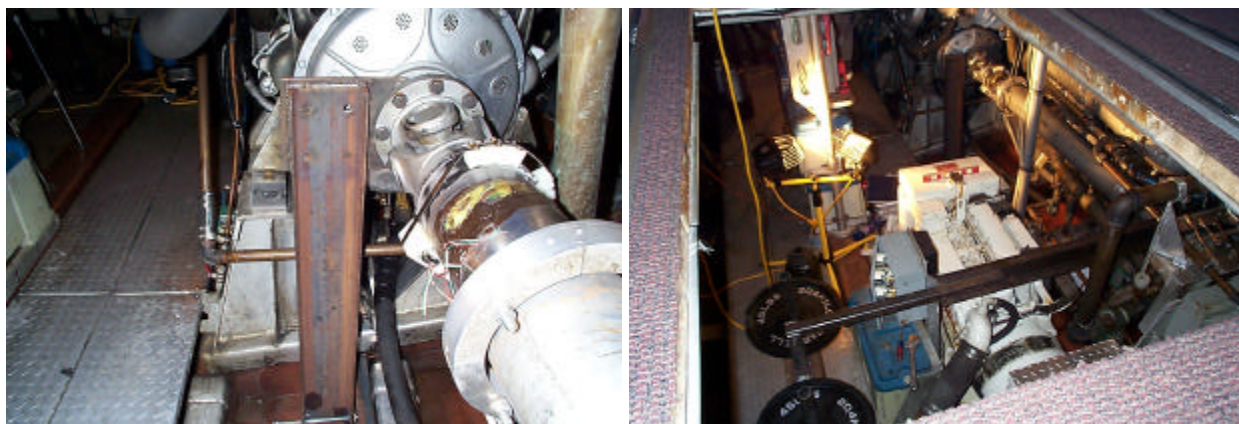


Figure 5 Load cell calibration arm and lock. The left photograph illustrates the shaft locking mechanism as shown in the middle of the picture. The right photograph illustrates the load arm extending from the shaft and over the generator. Weights were used to obtain different load points for the calibration curve.

It is noted that the shaft speed sensor was damaged beyond repair during the first day of testing. The cause of the damage was determined to be impact of the magnetic pickup against the RF collar on the rotating driveshaft. The magnetic sensor was rigidly attached to the engine frame and the mating sensor was placed on the drive shaft in the RF housing. It was determined that the fiberglass hull of the ferry distorted during high speed operation, resulting in a relative movement of the pickup and RF housing, causing the two to come into contact and breaking. Therefore, the engine tachometer on the dash of the bridge was used to determine engine speed, which was logged manually.

G. Additional Data

Additional data included the ambient pressure, temperature, and humidity. Vessel speed was also recorded from a Garmin GPS 35/36 unit to obtain speed over the water. It is recognized that GPS data does not provide sufficient information to relate engine load to vessel speed due to wind loading, water



current, or sea state. However, it does give some qualitative information about the test. These signals were recorded and stored into the WVU DAQ. Additionally, manual data were recorded from the vessel and included vessel GPS speed and the forward and aft starboard engine parameters of engine speed, oil pressure, water temperature, and intake (between turbocharger and supercharger) pressure on both banks. Additionally, the test engine's post turbocharger exhaust temperatures were recorded.

H. Instrumentation Control/Data Acquisition

Data acquisition was controlled with software developed by WVU. National Instruments E-series data acquisition boards with a minimum 12-bit resolution were used along with an SC-2345 signal conditioning unit. All analog data were recorded in raw voltage form at a minimum of 10 Hz and later converted to engineering units with a reduction program developed in-house at WVU. In addition, GPS data was recorded and stored to disk at 1 Hz.

Ferryboat Test Cycle

Steady-state engine operating points were utilized for the emissions testing. As noted above, the engine speed was reported from the panel mounted in the dash on the second deck. All testing was performed on the Pacific Ocean just offshore of Oceanside, CA. For the tests, nominal engine speeds of 1900, 2000, 2100 rpm and idle were selected as representative operating points. These points were selected since the ferry typically operates at 2100 rpm under calm conditions and between 1900 to 2100 rpm under rougher sea conditions. Sufficient vessel speed, associated with engine operation above 1900 rpm, was necessary for adequate hydrofoil operation. Idle conditions were also targeted since the engines idle during warm up, prior to leaving the dock, and after docking. To reiterate, testing was performed with baseline marine fuel and LSD fuel, as well as operation on each fuel with and without water injection. Table 2 details the test matrix. As shown in this table, a low speed marina configuration was included for the marine fuel. This point is the no-wake speed (idle with the transmission engaged) as the ferry enters or exits the marina.

It is noted that the 1900 rpm set point for the LSD fuel had a failure in the load cell for the torque measurement. Because of time constraints, this point was not repeated after the load cell was fixed. The reason for the failure was a broken solder connection between the strain gauge and the RF transmitter broke.

Repeats were performed at each engine set point. Due to the nature of in-use testing, it was nearly impossible to vary the load on the engine (or engines); the load applied to the engine was a function of the requirements set forth by the ferry operation (passenger loading, wind, current direction, speed, etc.). Therefore, the loading on the engine(s) could vary from set point-to-set point since no effort was made to reproduce the exact path of the ferry for each set point. However, engine speed is the primary variable in determining load. The data collection procedure consisted of operating the ferry at a constant engine speed for a short duration (~ five minutes). After the emissions had stabilized, data collection commenced. The duration of the data collection was dependant upon the PM filter loading. The test times were varied according to the expected filter loading and from examining the pressure drop across the filter.

Table 2 Test configuration set points.

Fuel	Engine Speed (rpm)	Water Injection	Comment
LSD	650 (Idle)	Off	
	1900	On	Failure of Torque Measurement
	2000	On / Off	
	2100	On / Off	
Marine	650 (Idle)	Off	
	650 (Marina)	Off	
	1900	On / Off	
	2000	On / Off	
	2100	On / Off	

Data Reduction Methodology

The research performed for this study involved in-use emissions evaluation from an engine in a marine vessel. Although there are no specific standards that outline procedures for testing of this nature, data reduction procedures outlined in Title 40 CFR 86, Title 40 CFR 89, Title 40 CFR 92, Title 40 CFR 94, ISO8178, and SAE J177 were followed, where applicable, in the experimental setup and data evaluation [2-7]. The computation of the mass emissions emitted from the engine in the ferry can be determined from the sources listed above. Generally, knowledge of the intake air flow rate and fuel flow rate (or exhaust flow rate) and the concentration level of the exhaust constituents are required. The method of reporting the mass flow through the engine used for this work was direct intake flow with a laminar flow meter.

Mass rates of each exhaust constituent were determined from associated measured concentration levels in the exhaust and measured fuel mass flow rates, as defined in Title 40 CFR 92 [4]. The data from the last 60 seconds of each steady-state point were averaged and used for the gaseous emission analysis. For PM, the entire duration of the sampling period was used for the determination of the TPM. The emission mass rate may be calculated using the concentration levels reported on a wet basis, neglecting carbon monoxide and total hydrocarbons, is given by

$$\dot{M}_i = \frac{\dot{M}_f * C_{i,w} * MW_i}{(12.011 + 1.008 * a) * (C_{CO_2,w})} \quad (1)$$

or reported on a dry basis

$$\dot{M}_i = \frac{\dot{M}_f * C_{i,d} * MW_i}{(12.011 + 1.008 * a) * (C_{CO_2,d})} \quad (2)$$

The molecular weight of each constituent is shown in Table 3. The dry and wet concentration levels are related by

$$C_{i,d} = K_w * C_{i,w} \quad (3)$$



where the correction factor is given as

$$K_w = 1 + D_{H_2O} . \quad (4)$$

The value of D_{H_2O} can be determined from an iterative process or using an approximate solution. An approximate solution used in this analysis and is given by:

$$D_{H_2O} = \left[\frac{a * C_{CO_2,d}}{2} + Y * DVOL_{Ratio} \right], \quad (5)$$

where

$$DVOL_{Ratio} = 1 - \left(\frac{a}{4} \right) * C_{CO_2,d} . \quad (6)$$

The constituent CO_2 was measured dry, while NO_x was measured wet. Equation (2) was used for calculating the mass emission rate.

Table 3 Molecular weight of each exhaust constituent.

Constituent i	MW
CO_2	44.01
NO_x^*	46.01

* NO_x molecular weight based on NO_2 , per CFR requirements

The mass emission rate of NO_x was corrected for ambient temperature and humidity according to procedure outlined in Title 40 CFR 89 [3].

The particulate matter mass rate was determined from knowledge of the partial flow dilution tunnel dilution ratio, particulate filter net mass, integrated flow across the filter during the test, and the average exhaust flow rate. The particulate matter mass rate is analogous to that given in ISO8178 [6] and is given by

$$\dot{M}_{PM} = \frac{m_{net} * \dot{Q}_{Exh}}{Q_{SecTun}} . \quad (7)$$

The flow across the filter was determined from integrating the measured flow through the mass flow controller on the mini dilution tunnel. The net filter mass was the sum of the PM loading on the primary and secondary filter. The average exhaust flow rate was determined from the measured in-field method.

The average exhaust volumetric flow rate over the PM collection phase was determined from the equivalence ratio, stoichiometric air-to-fuel ratio, and fuel flow measurement. The exhaust volumetric flow rate is given as

$$\dot{Q}_{Exh} = r * \dot{M}_{Exh} \quad (8)$$

where the exhaust mass rate is given as



$$\dot{M}_{Exh} = \dot{M}_{intake} + \dot{M}_{fuel} \quad (9)$$

The brake specific mass emission for each exhaust constituent was determined by

$$bs_i = \frac{\dot{M}_i}{P}, \quad (10)$$

where the power was determined from the measured propeller shaft speed and torque and is given as

$$P = \frac{T * N}{5252} \quad (11)$$

Results

The results from the research are presented in tabular format in Table 4 to Table 8 and in graphical format in Figure 6 to Figure 11. Fuel analysis for the two fuels used in the study is given in Table 9 and the oil analysis from the test engine is given in Figure 12 and Figure 13. The oil analysis has identified potential problems with the engine and should be examined by the owners in more detail.

Care must be exercised when reviewing the data for the low sulfur fuel (LSD). The fuel analysis for the “BP ECD[®]” fuel shows very high (320 ppm) sulfur concentration. It was possible that during the fuel extraction from the tank that the sample was contaminated due to the piping configuration connecting the two tanks. However, the sampling line was purged before the sample was collected and is not believed to be the source of contamination. The ferry had what appeared to be two separate tanks. It was confirmed through subsequent testing by the operator that the two tanks were indeed fully separated and that sloshing should not have occurred from the tank with the marine fuel to the tank containing the low sulfur diesel. Another possible source of contamination could have been from the process of purging the tank used for the low sulfur fuel. Prior to emissions testing, a plan was developed to fill both tanks with low sulfur. Approximately a week before the emissions testing, the port tank was filled with marine fuel. The starboard engines were then fueled with the low sulfur fuel and the port engines were fueled with the marine fuel. The ferry was then operated over its normal service and the two tanks filled with their respective fuels. Hence, at each refilling, the contamination level in each tank would diminish.

Table 4 displays the manual data collected from the forward and aft starboard engines. As illustrated in this table, the forward and aft engines appear to have been operating at a similar load as indicated by the engine speed, oil pressure, water temperature, and turbocharger pressure. It is noted that the one exhaust temperature (T2) on the test engine malfunctioned and was not recorded – these tabular entries are highlighted. Other data points not recorded are also highlighted. It is observed that the exhaust temperatures were typically lower when the water injection system was active than when the water injection system was disabled. This is attributed to the fact that lower in-cylinder temperatures were obtained with the water injection. This is also supported by the lower NO_x emissions. The exhaust temperature data for the harbor runs may appear to be confusing. As shown for M010126-1 and M010130-1 the temperatures continued to drop throughout the testing. This is due to the fact that the ferry was entering the marina from the ocean at full power and the engine was at normal operating temperature. The engine coolant and oil began to cool during these tests. However, the temperature for the other harbor run, M010127-1, was for the ferry leaving the dock, thus the engine was at its normal idle operating temperature and did not change during the test since there was minimal load on the engine.



Table 5 and Table 7 illustrate the individual run data for the vessel underway and at the dock, respectively. Table 6 and Table 8 are the average data from Table 5 and Table 7 for the vessel underway and at the dock, respectively. The average data from Table 6 and Table 8 are plotted in Figure 6 to Figure 9. The bars in these graphs represent one standard deviation of the data. Care must be exercised in using the standard deviation since only a limited number of repeats were performed and the nature of in-use emissions testing dictates that repeat runs are difficult to achieve. However, the spread of the data does allow for a discussion of the variability of the data. Figure 10 compares the average reduction in the emissions due to the water injection system and Figure 11 illustrates the average reduction in the emissions due to the switch of the fuels from conventional marine to a low sulfur, lower aromatic, higher cetane fuel.

From Figure 6, the average power for each test condition was repeatable. The data in this figure was influenced by the ocean and weather conditions, although there were no noticeable differences during the two days of testing. The greatest difference between the set point occurred for the 2000 rpm set point, an averaged difference of only 1.2%. From the data, it is difficult to determine if there was a cubic relationship between the shaft speed and engine power for the vessel's water jet propulsion system as would be found in conventional propeller propulsion systems, but the vessel operators indicated that for the jet system the relationship was more linear than that for a direct propeller system.

The brake-specific fuel consumption, Figure 7, is consistent at approximately 0.4 lb/bhp-hr for either fuel and with or without water injection. For the harbor tests with the marine fuel, the brake fuel consumption was dramatically higher due to low engine speed (650 rpm) and low power output. There does not appear to be a fuel penalty associated with using the low sulfur fuel or the water injection system

The brake-specific mass emissions of NO_x and PM in Figure 8 and Figure 9, respectively, and in the comparisons in Figure 10 and Figure 11 shows that the PM is reduced by approximately 40% from the marine fuel to the low sulfur fuel while the vessel was underway. It is noted that there is a relatively large variation in the PM data for the 2100 rpm set point. There may be a slight PM reduction when using the water injection system but it is not seen as being significant and is within the uncertainty of the experimental procedure. A significant reduction in NO_x is seen when the water injection system was used. The water injection system was activated only when the boost pressure was above a certain limit. Therefore, only the higher load set points had the water injection system activated. As seen in these two figures, the LSD fuel with water injection had a slightly higher reduction percentage than that of the marine fuel for a given set point. Also, there is a larger reduction percentage at lower engine speeds. This is due to the fact that there was a higher percentage of water injected at the lower engine speeds due to a constant water mass being injected when the system was activated. That is, there was no feedback or control on the amount of water injected into the intake; it was either on or off. The percentages shown in Figure 11 for idle should be used with caution. There is uncertainty in the data at idle due to the measurement equipment and the procedures used. Further testing would be warranted to draw any conclusive arguments on the idle data. Unfortunately, the uncertainty in the idle data was not found until after the testing was completed and it was not possible to retest the engine at idle due to budget constraints.

Conclusions

This effort evaluated the in-field mass rate and brake-specific mass emissions of NO_x and PM and fuel consumption for a high-speed ferry operating between Oceanside and San Diego, CA. For the water injection system, the brake-specific mass emissions of NO_x were reduced by 16.5 % and PM emissions



were reduced by 40% using low sulfur diesel fuel and water injection compared to marine fuel. However, there is some uncertainty in the low sulfur fuel composition in that the low sulfur diesel fuel (BP ECD[®]) was contaminated at some point during the testing and was not at the desired low sulfur level for the test. However, it should be recognized that even with this uncertainty, the low sulfur diesel fuel that was tested had at least an order of magnitude lower sulfur level than the baseline marine fuel.

Acknowledgements

The author acknowledges the dedicated support of organizations and individuals. Firstly, the US Department of Energy Office of Transportation Technology is thanked for providing the financial support and Stephen Goguen of the US Department of Energy, Office of FreedomCAR & Vehicle Technologies, is thanked for his support of the program. Bob Behr and Danny Gore from the Maritime Administration are thanked for providing technical support related to marine issues. Michael Winn and Lou Adamo from SCX, Inc are thanked for their logistical support. Ken Kimura at BP is thanked for providing the low sulfur diesel fuel. Anatoly Mezheritsky at M.A. Turbo/Engines is thanked for the installation of the water injection system. The Marine Services Express crew are acknowledged for their effort on pulling off the testing: Phillip Winter, captain Jim Saffer, mate Matt Hallisey, engineer Matt Rowley, and deckhand John Vierling. Finally, the faculty, staff, and students at West Virginia University are thanked for providing the extra effort for this work.

Table 4 Manual data collected from starboard forward and aft engines. Note that the 1900 rpm with LSD and WIS data were not collected. The horizontal line represents the two different test days.
The data are also shown in the sequence in which it were collected.

Description	Seq No	Run No	GPS Spd knts	Forward Starboard Engine						Aft Starboard Engine					
				Eng Spd	Oil Pres	Water Temp	Exh Temp		Turbo Pres		Eng Spd	Oil Pres	Water Temp	Turbo Pres	
				RPM	psig	F	T1	T2	P1	P2	RPM	psig	F	P3	P4
2100 rpm, LSD	M010113	2		2100	60	180	635		18.7	19.2	2100	60	180	19.2	19.9
2100 rpm, LSD	M010113	3	37.0	2100	60	180	631		18.8	19.3	2100	60	180	19.0	19.4
2100 rpm, LSD, WIS	M010114	1	36.0	2100	60	180	617		18.9	19.3	2100	60	180	19.3	19.6
2100 rpm, LSD, WIS	M010114	2	33.6	2100	60	180	618		18.9	19.4	2100	60	180	19.1	19.6
2000 rpm, LSD, WIS	M010115	2	30.3	2000	60	180	600		15.8	16.2	2000	60	180	15.4	16.0
2000 rpm, LSD, WIS	M010115	3	32.6	2000	60	180	600		15.6	16.1	2000	60	180	15.2	15.8
2000 rpm, LSD	M010116	1	30.3	2000	60	180	-		15.3	15.6	2000	60	180	15.2	15.9
2000 rpm, LSD	M010116	2	28.8	2000	60	180	627		15.5	15.7	2000	60	180	15.1	15.6
1900 rpm, LSD	M010117	1	24.4	1900	60	170	600		12.3	12.6	2000	60	170	12.0	12.5
Idle, 650 rpm, LSD	M010118	1	0.0	670	25	120	137		0.1	0.1	670	25	120	0.2	0.2
Idle, 650 rpm, LSD	M010118	2	0.0	670	25	115	137		0.1	0.1	670	25	115	0.2	0.2
2100 rpm, Marine	M010119	1	35.6	2100	60	180	636		19.5	19.9	2100	60	180	19.8	20.2
2100 rpm, Marine	M010119	2	34.0	2100	60	180	632		18.7	19.2	2100	60	180	19.0	19.7
2100 rpm, Marine, WIS	M010120	1	33.0	2100	60	180	625		19.2	19.7	2100	60	180	19.7	20.3
2100 rpm, Marine, WIS	M010120	2	33.8	2100	60	180	621		19.4	19.8	2100	60	180	19.7	20.2
2000 rpm, Marine, WIS	M010121	1	28.6	2000	60	180	600		15.7	16.1	2000	60	180	15.1	15.9
2000 rpm, Marine, WIS	M010121	2	30.0	2000	60	180	597		15.7	16.2	2000	60	180	15.2	15.8
2000 rpm, Marine	M010122	1	29.2	2000	60	180	615		15.6	15.9	2000	60	180	15.3	15.9
2000 rpm, Marine	M010122	2	30.0	2000	60	180	617		15.5	15.9	2000	60	180	15.2	15.9
1900 rpm, Marine	M010123	1	25.5	1900	60	180	600		12.5	12.8	1900	60	180	12.5	12.5
1900 rpm, Marine	M010123	2	24.7	1900	60	180	602		12.5	12.8	1900	60	180	12.4	12.4
1900 rpm, Marine, WIS	M010124	1	25.0	1900	60	180	585		12.8	13.1	1900	60	180	12.3	12.3
1900 rpm, Marine, WIS	M010124	2	27.8	1900	60	180	585		12.8	13.1	1900	60	180	12.3	12.3
2100 rpm, Marine, WIS	M010125	1	32.2	2100	60	180	625		19.1	19.5	2100	60	180	19.1	19.1
650, Marine, Harbor, Temperature dropped through test	M010126	1	5.5	650	25	170	275-235		0.2	0.2	650	25	175	0.1	0.1
650, Marine, Harbor	M010127	1	3.2	650	25	125	190		0.2	0.1	650	25	125	0.3	0.3
2100 rpm, Marine, WIS	M010128	1	37.0	2100	60	180	620		19.2	19.5	2100	60	180	19.5	20.0
2100 rpm, Marine, WIS	M010128	2	35.5	2100	60	180	630		19.2	19.9	2100	60	180	19.7	20.1
2100 rpm, Marine, WIS	M010128	3	36.0	2100	60	180	628		19.3	20.0	2100	60	180	19.7	20.0
2100 rpm, Marine	M010129	1	31.5	2100	60	180	636		18.9	19.5	2100	60	180	19.2	19.7
2100 rpm, Marine	M010129	2	31.3	2100	60	180	636		19.0	19.5	2100	60	180	19.0	19.6
2100 rpm, Marine	M010129	3	31.8	2100	60	180	637		19.1	19.5	2100	60	180	19.0	19.7
650, Marine, Harbor, Temperature dropped through test	M010130	1	4.3	650	15	170	282-240		0.2	0.2	650	15	170	0.3	0.3
Idle, 650, Marine	M010131	1	0.0	650	12	120	143		0.5	0.5	650	0	0	0.0	0.0
Idle, 650, Marine	M010131	2	0.0	650	12	120	140		-	-	650	0	0	0.0	0.0

Table 5 Individual run data for each configuration while underway. Note that the 1900 rpm with LSD and WIS data were not collected.

Run No.	Fuel	Comment	Engine Speed rpm	GPS Speed mph	GPS Speed mph	Power hp	BSNOx g/bhp-hr	BSFC lb/bhp-hr	BSPM g/bhp-hr
M01 0113 - 2	LSD	2100 rpm LSD	2100	40.2	0.0	854	6.67	0.403	0.112
M01 0113 - 3	LSD	2100 rpm LSD	2100	39.5	42.6	855	6.77	0.404	0.086
M01 0114 - 1	LSD	2100 rpm LSD WIS	2100	39.6	41.4	851	5.91	0.402	0.096
M01 0114 - 2	LSD	2100 rpm LSD WIS	2100	38.0	38.7	853	5.97	0.405	0.096
M01 0119 - 1	CA Marine	2100 rpm Marine	2100	38.4	41.0	866	6.91	0.410	0.159
M01 0119 - 2	CA Marine	2100 rpm Marine	2100	38.7	39.1	850	7.18	0.405	0.140
M01 0129 - 1	CA Marine	2100 rpm Marine	2100	35.1	36.2	860	7.25	0.406	0.184
M01 0129 - 2	CA Marine	2100 rpm Marine	2100	36.4	36.0	855	7.22	0.407	0.182
M01 0129 - 3	CA Marine	2100 rpm Marine	2100	35.4	36.6	854	7.17	0.407	0.187
M01 0120 - 1	CA Marine	2100 rpm Marine WIS	2100	37.5	38.0	856	6.25	0.408	0.149
M01 0120 - 2	CA Marine	2100 rpm Marine WIS	2100	38.4	38.9	860	6.33	0.410	0.147
M01 0125 - 1	CA Marine	2100 rpm Marine WIS	2100	37.6	37.1	844	5.97	0.410	0.210
M01 0128 - 1	CA Marine	2100 rpm Marine WIS	2100	41.4	42.6	859	6.66	0.410	0.166
M01 0128 - 2	CA Marine	2100 rpm Marine WIS	2100	40.9	40.9	861	6.65	0.410	0.177
M01 0128 - 3	CA Marine	2100 rpm Marine WIS	2100	40.2	41.4	863	6.66	0.409	0.179
M01 0116 - 1	LSD	2000 rpm LSD	2000	34.9	34.9	738	6.51	0.401	0.114
M01 0116 - 2	LSD	2000 rpm LSD	2000	35.9	33.1	738	6.39	0.393	0.109
M01 0115 - 2	LSD	2000 rpm LSD WIS	2000	35.3	34.9	739	5.56	0.402	0.104
M01 0115 - 3	LSD	2000 rpm LSD WIS	2000	36.5	37.5	736	5.46	0.400	0.105
M01 0122 - 1	CA Marine	2000 rpm Marine	2000	33.6	33.6	731	6.47	0.402	0.195
M01 0122 - 2	CA Marine	2000 rpm Marine	2000	34.7	34.5	730	6.53	0.402	0.189
M01 0121 - 1	CA Marine	2000 rpm Marine WIS	2000	33.6	32.9	729	5.69	0.402	0.175
M01 0121 - 2	CA Marine	2000 rpm Marine WIS	2000	33.0	34.5	732	5.67	0.401	0.182
M01 0117 - 1	LSD	1900 rpm LSD	1900	28.8	28.1	620	5.97	0.399	0.160
M01 0123 - 1	CA Marine	1900 rpm Marine	1900	28.3	29.3	620	5.94	0.405	0.264
M01 0123 - 2	CA Marine	1900 rpm Marine	1900	29.2	28.4	620	5.94	0.405	0.256
M01 0124 - 1	CA Marine	1900 rpm Marine WIS	1900	28.2	28.8	621	4.94	0.405	0.246
M01 0124 - 2	CA Marine	1900 rpm Marine WIS	1900	31.7	32.0	621	4.98	0.405	0.246
M01 0126 - 1	CA Marine	650 rpm Harbor Marine	650	4.6	6.3	21	16.79	0.874	0.165
M01 0127 - 1	CA Marine	650 rpm Harbor Marine	650	3.9	3.7	20	20.78	0.970	0.162
M01 0130 - 1	CA Marine	650 rpm Harbor Marine	650	4.7	4.9	22	17.68	0.844	0.149

Table 6 Averaged run data for each configuration while underway. Note that the 1900 rpm LSD with WIS data were not collected.

Comment	Engine Speed rpm	GPS Speed mph	GPS Speed mph	Power hp	BSNOx g/bhp-hr	BSFC lb/bhp-hr	BSPM g/bhp-hr
2100 rpm LSD	2100	39.9	21.3	854.4	6.717	0.403	0.099
2100 rpm LSD WIS	2100	38.8	40.0	852.2	5.940	0.404	0.096
2100 rpm Marine	2100	36.8	37.8	857.0	7.145	0.407	0.170
2100 rpm Marine WIS	2100	39.3	39.8	857.1	6.420	0.409	0.171
2000 rpm LSD	2000	35.4	34.0	737.7	6.451	0.397	0.112
2000 rpm LSD WIS	2000	35.9	36.2	737.7	5.512	0.401	0.105
2000 rpm Marine	2000	34.2	34.1	730.9	6.499	0.402	0.192
2000 rpm Marine WIS	2000	33.3	33.7	730.4	5.679	0.402	0.179
1900 rpm LSD	1900	28.8	28.1	620.4	5.969	0.399	0.160
1900 rpm ECD WIS							
1900 rpm Marine	1900	28.7	28.9	620.0	5.939	0.405	0.260
1900 rpm Marine WIS	1900	30.0	30.4	620.8	4.960	0.405	0.246
650 rpm Harbor Marine	650	4.4	5.0	20.9	18.416	0.896	0.159

Table 7 Individual run data for each configuration while idle at the dock. Note that the 1900 rpm with LSD and WIS data was not collected.

Run No.	Fuel	Comment	Engine Speed rpm	GPS Speed mph	GPS Speed mph	Power hp	NOx g/hr	FC lb/hr	PM g/hr
M01 0118 - 1	LSD	LSD Idle	670	0.0	0.0	0	210.59	12.170	1.232
M01 0118 - 2	LSD	LSD Idle	670	0.0	0.0	0	211.33	12.209	1.376
M01 0131 - 1	CA Marine	Marine Idle	650	0.0	0.0	0	175.74	10.548	3.251
M01 0131 - 2	CA Marine	Marine Idle	650	0.0	0.0	0	173.56	11.046	5.638

Table 8 Averaged run data for each configuration while idle at the dock.

	Engine Speed rpm	GPS Speed mph	GPS Speed mph	Power hp	BSNOx g/hr	BSFC lb/hr	BSPM g/hr
LSD Idle	670	0	0	0	211	12.19	1.304
Marine Idle	650	0	0	0	175	10.80	4.445

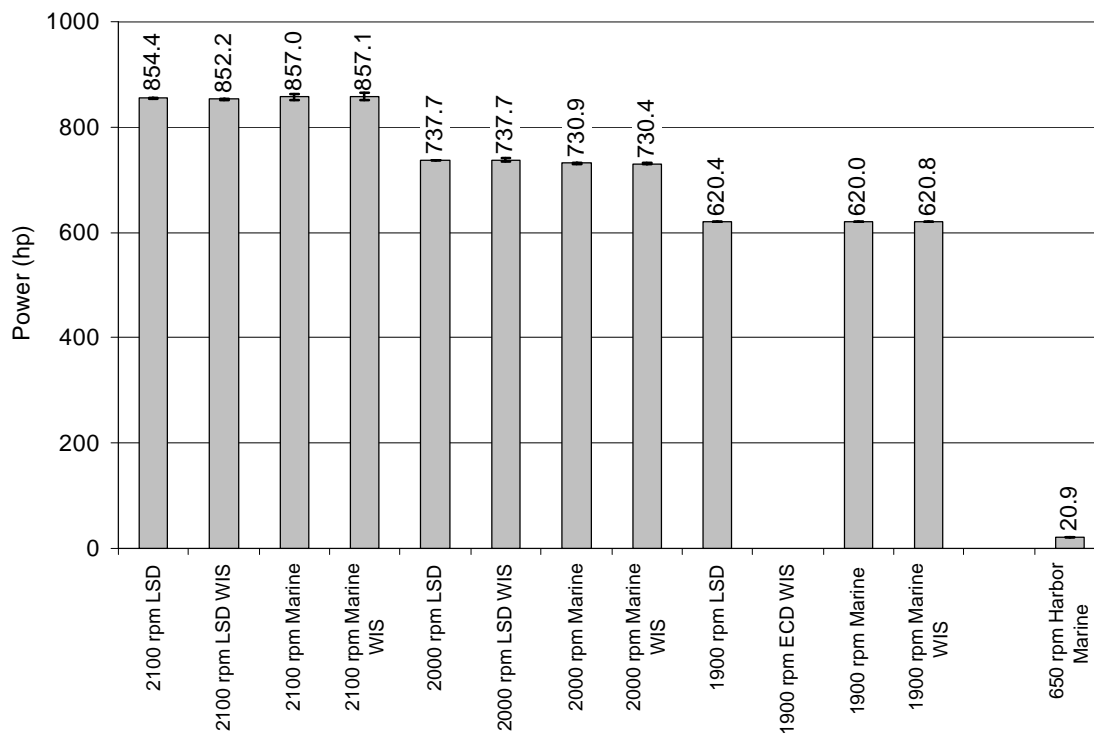


Figure 6 Average power for each test configuration. Note that the 1900 rpm with LSD and WIS data were not collected.

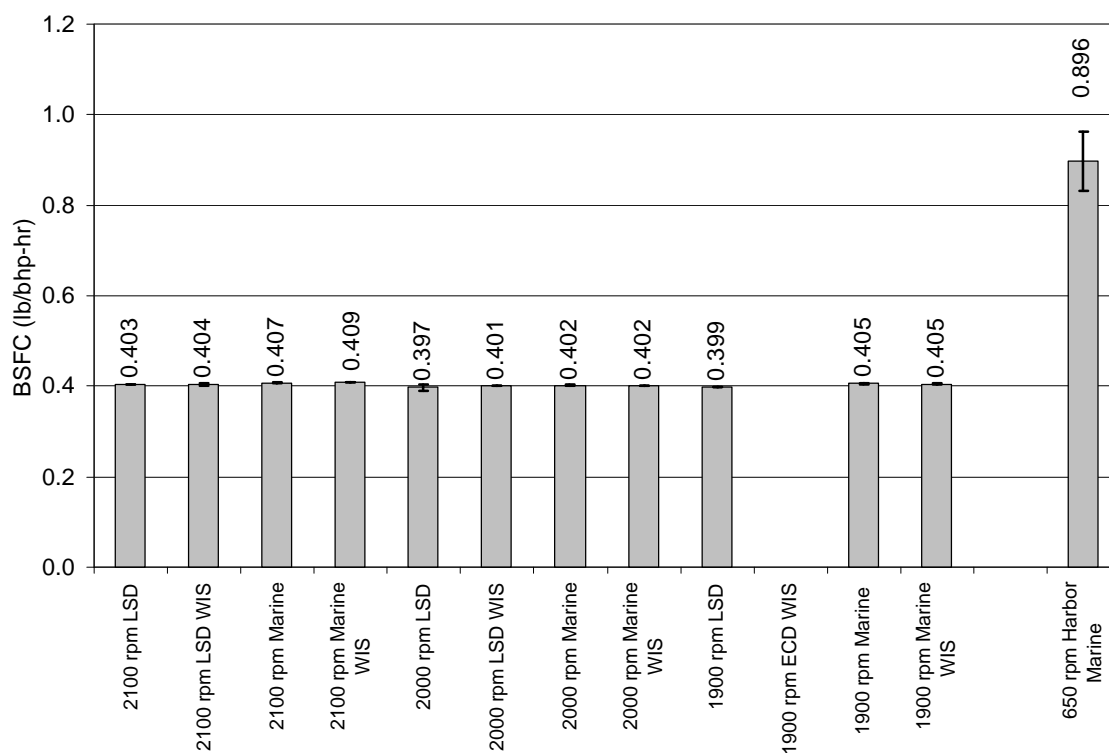


Figure 7 Average brake-specific fuel consumption. Note that the 1900 rpm with LSD and WIS data were not collected.

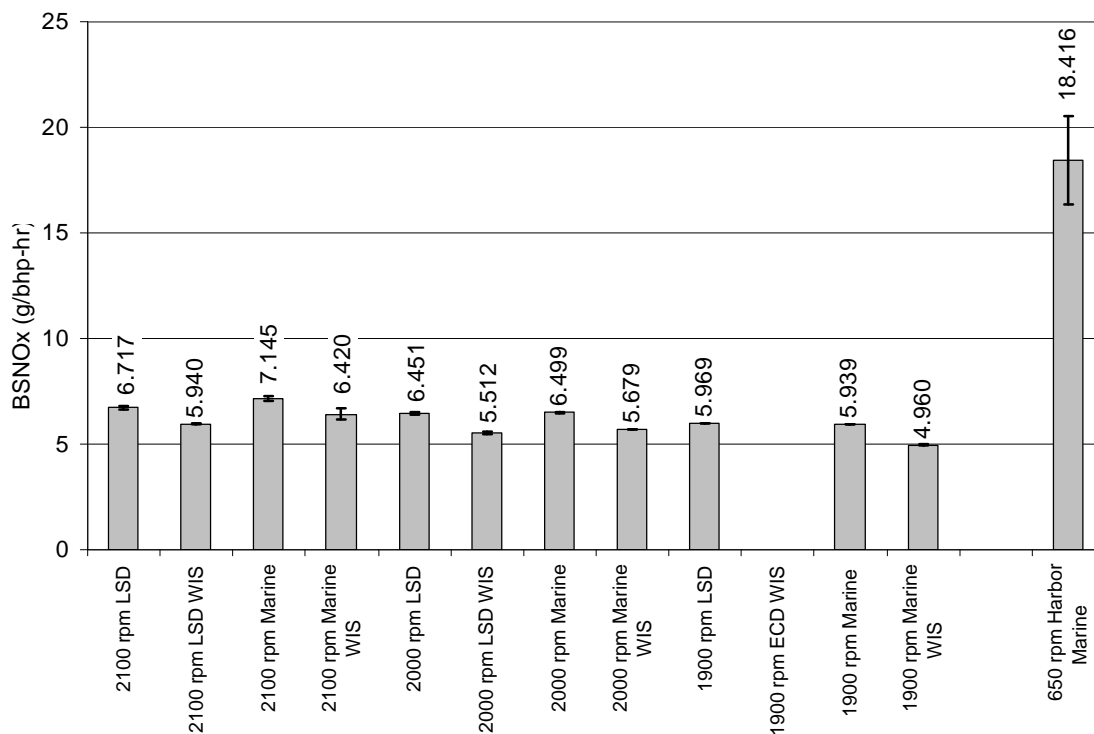


Figure 8 Average brake-specific NOx emissions. Note that the 1900 rpm with LSD and WIS data were not collected.

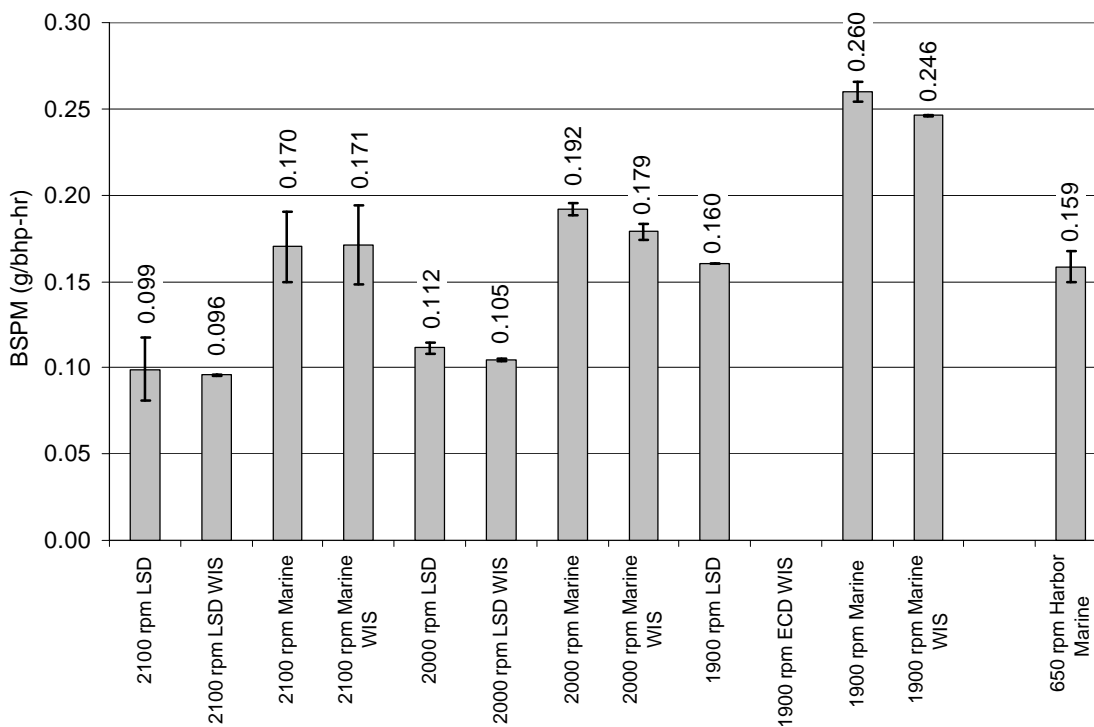


Figure 9 Average brake-specific PM emissions. Note that the 1900 rpm with LSD and WIS data were not collected.

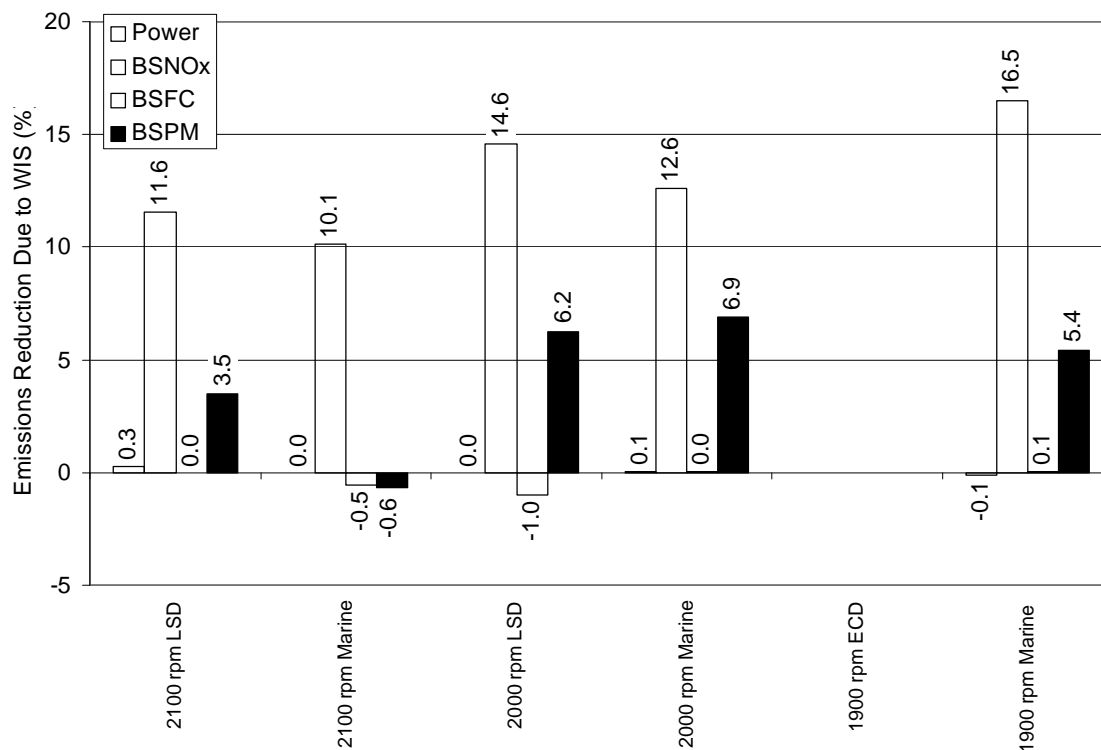


Figure 10 Emissions reduction due to water injection. Note that the 1900 rpm with LSD and WIS data were not collected.

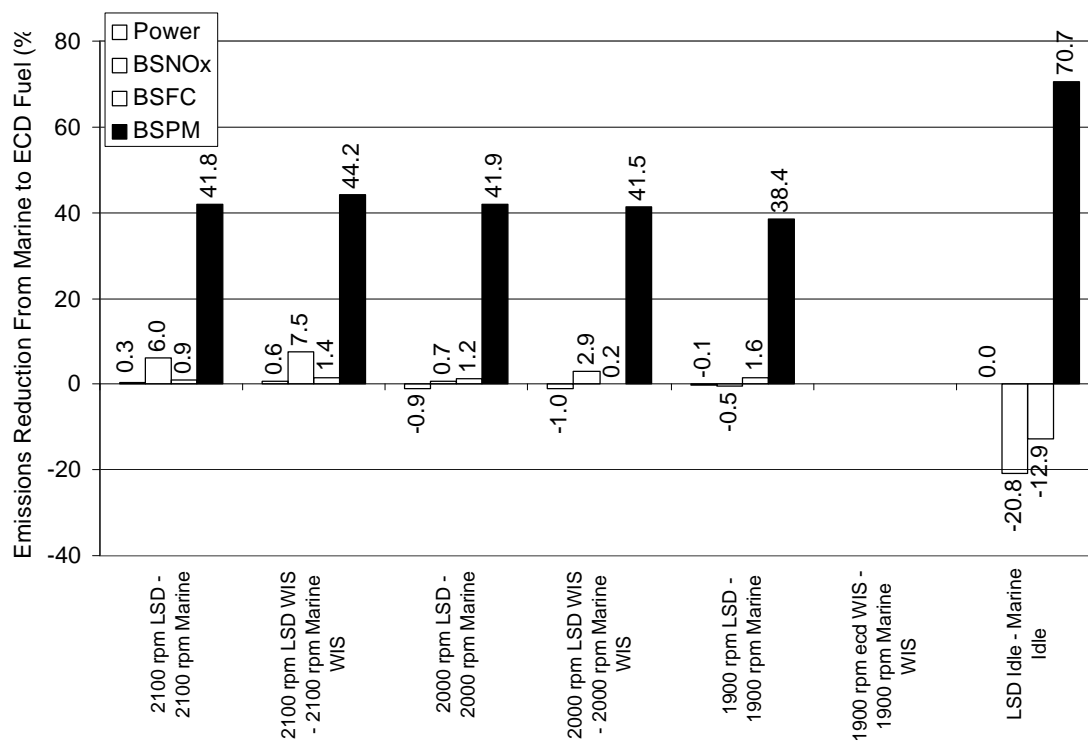


Figure 11 Emissions reduction between marine and LSD fuel change. Note that the 1900 rpm with LSD and WIS data were not collected.



References

- 1 M.A. Turbo/Engine, Ltd., Vancouver, BC.
- 2 *Title 40 Code of Federal Regulations, Part 86*, U.S. Government Printing Office, Washington, DC, 2000.
- 3 *Title 40 Code of Federal Regulations, Part 89*, U.S. Government Printing Office, Washington, DC, 2000.
- 4 *Title 40 Code of Federal Regulations, Part 92*, U.S. Government Printing Office, Washington, DC, 2000.
- 5 *Title 40 Code of Federal Regulations, Part 94*, U.S. Government Printing Office, Washington, DC, 2000.
- 6 "Reciprocating Internal Combustion Engines – Exhaust Emissions Measurement", International Organization for Standardization, ISO/DIS 8178, Geneva, Switzerland, 1993.
- 7 "Measurement of Carbon Dioxide, Carbon Monoxide, and Oxides of Nitrogen in Diesel Exhaust," 6SAE Standard, SAE J177, Warrendale, PA 1995.
- 8 Gautam, M., Clark, N. N., Thompson, G. J., and Lyons, D. W., "Assessment of Mobile Monitoring Technologies for Heavy-Duty Vehicle Emissions," Whitepaper Submitted to the Settling Heavy-Duty Diesel Engine Manufacturers, Department of Mechanical and Aerospace Engineering, West Virginia University, Morgantown, WV, 1999. See:
<http://www.epa.gov/Compliance/civil/programs/caa/diesel/test.html>.
- 9 Gautam, M., Clark, N. N., Thompson, G. J., Carder, D. K., and Lyons, D. W., "Evaluation of Mobile Monitoring Technologies for Heavy-Duty Diesel-Powered Vehicle Emissions," Phase I Final Report Submitted to the Settling Heavy-Duty Diesel Engine Manufacturers, Department of Mechanical and Aerospace Engineering, West Virginia University, Morgantown, WV, 2000. See:
<http://www.epa.gov/Compliance/civil/programs/caa/diesel/test.html>.
- 10 Gautam, M., Clark, N. N., Thompson, G. J., Carder, D. K., and Lyons, D. W., "Development of In-use Testing Procedures for Heavy-Duty Diesel-Powered Vehicle Emissions," Phase II Final Report Submitted to the Settling Heavy-Duty Diesel Engine Manufacturers, Department of Mechanical and Aerospace Engineering, West Virginia University, Morgantown, WV, 2000. See:
<http://www.epa.gov/Compliance/civil/programs/caa/diesel/test.html>.
- 11 Gautam, G., Thompson, G. J., Carder, D. K., Clark, N. N., Shade, B. C., Riddle, W. C., and Lyons, D. W., "Measurement of In-Use, On-Board Emissions from Heavy-Duty Diesel Vehicles: Mobile Emissions Measurement System," SAE Technical Paper No. 2001-01-3643, 2001.



Appendix - Fuel and Oil Sample Data Sheets

Table 9 SCX diesel fuel analysis report. The LSD fuel, BP ECD[®], may have been contaminated. Care must be exercised when referencing this data to note this potential contamination.

Test	Units	Method	Fuel	
			LSD	Marine
API Gravity @ 60 Deg. F	deg.API	ASTM D-1298	39.2	34.7
Carbon	wt%	ASTM D-5291M	86.36	86.49
Cetane Index, Calculated	-	ASTM D-976	51.8	47
Cetane Number	-	ASTM D-613	53.1	46.1
Hydrogen Content	wt%	ASTM D-5291M	13.56	13.42
Kinematic Viscosity @ 40 deg. F	cSt	ASTM D-445	3.33	2.7
Specific Gravity	@ 60 deg.F	ASTM D-1298	0.8289	0.8514
Total Sulfur	wt%	ASTM D-4294	0.032	0.394
Distillation				
IBP	deg.F	ASTM D-86	365.6	347.9
5% Rec	deg.F		389.4	390.4
10% Rec	deg.F		401.2	413.4
20% Rec	deg.F		424.8	444.5
30% Rec	deg.F		447.3	469
40% Rec	deg.F		467.8	492
50% Rec	deg.F		492.1	514.1
60% Rec	deg.F		517.1	536.6
70% Rec	deg.F		542.8	559.7
80% Rec	deg.F		574.3	54.3
90% Rec	deg.F		612.5	623.3
95% Rec	deg.F		644.9	664.4
FBP	deg.F		667.2	676.4
Recovery	%		98.2	97.6
Residue	%		1.5	1.2
Loss	%		0.3	1.3
Flash Point, PMCC	deg.F	ASTM D-93(A)	140	136
Hydrocarbon Type - FIA				
Aromatics	lv%	ASTM D-1319	21.8	27
Olefins	lv%		0.8	0.7
Saturates	lv%		77.4	72.3



OIL SCIENCE LABORATORY

3940 Marine Avenue, Suite L, El Camino Village • Lawndale, California 90260-2333
Phone: 1-800-313-5555 • (310) 676-5951 • Fax: (310) 676-5952

June 11, 2003

Mechanical & Aerospace Engineering
West Virginia University
PO Box 6101
Morgantown, WV 26506

Samples: Stbd Engine, SCX Ferry. Type: Diesel engine oil.
ASTM D4294, Sulfur content by X-ray.

LABORATORY RESULTS

Sample #

Sulfur, wt%

Stbd Engine, SCX Ferry

0.5350

Sulfur content is consistent with diesel engine lubricating oil.
note: results are in wt/wt percentage. 0.1 wt% is equivalent to 1,000 ppm.

Paul N Rollins

Quality assurance in inspection and test.

Figure 12 SCX starboard engine oil analysis result.



O I L S C I E N C E R E P O R T

CUSTOMER ACCOUNT NO: 526
West Virginia University
M and A Engineering
PO Box 6101
Morgantown, WV 26506

LUBE BRAND:
LUBE TYPE: motor, del
TOTAL MILS/HOURS: 0

UNIT ID: 8TBD-SCX DATE: 06/11/03
SYSTEM: Starboard engine, SCX
COMP/MFG: Ferry
PO: prepay FUEL: diesel
WARRANTY:

ATTN: Thomas K Spencer
PHONE: 304-2932419

[NOTE: * = OILSCIENCE PROPRIETARY VALUES: (NORMAL: 1 OR 2, ABNORMAL: 3, SEVERE: 4.)]

Test No:	000526-00008
Date Sampled:	04/27/03
Date Received:	06/04/03
Iron ppm	174
Chromium ppm	30
Zinc ppm	1462
Aluminum ppm	2
Manganese ppm	2
Tin ppm	8
Phosphorus ppm	1076
Calcium ppm	715
Nickel ppm	<1
Copper ppm	16
Lead ppm	9
Boron ppm	165
Silicon ppm	17
Sodium ppm	38
Barium ppm	<1
Magnesium ppm	1007
Titanium ppm	<1
Viscosity (SAE)	30
Viscosity (SUS)	526
Viscosity *	2
Fuel Dilution *	2
Coolant Leak *	2
Sludge K	2.13
Soot *	3
Particulates *	3
Migration *	2
Oxidation *	2
New Oil *	2
Lube Drain	
Total Mi/Hrs	
Sample Mi/Hrs	

TEST NUMBER: 000526-00008

- EVALUATIONS: Abnormal iron/steel wear, and chromium wear. These indicate advanced wear of the cylinder liners, piston rings; top end. Tin, bearing overlay, above normal but appears secondary, due to stress on the bearings from the top end condition. Minor soot, but appears related to top end condition, rather than another problem. Water absent. Conditions other than the above are normal. (note: zinc, phosphorus, calcium, magnesium are normal additives). Sulfur result is attached.

- ACTION: High iron and chromium signify top end problem. Compression test advised to identify bad/worn cylinder(s). Correction of this should result in a strongly running engine.

OILSCIENCE (310) 676-5951. 3940 Marine Ave, Suite L, El Camino Village, Lawndale, CA 90260

Figure 13 SCX starboard engine oil analysis result.